4. J. G. Marvin and Y. S. Sheaffer, A method for solving nonsimilar laminar boundary-layer equations including foreign gas injection, NASA TN D-5516 (1969).
5. C. S. Vimala and G. Nath, Unsteady laminar boundary layers in a compressible stagnation flow, *J. Fluid Mech.* **70**, 561–572 (1975).
6. W. L. Bade, Stagnation-point heat transfer in a high-temperature inert gas, *Phys. Fluids* **5**, 150–154 (1962).
7. J. F. Gross and C. F. Dewey, Similar solutions of the laminar boundary layer equations with variable properties, *Fluid Dynamics Transactions* Vol. 2, p. 529. Pergamon Press, Oxford (1965).
8. R. J. Gribben, The fluctuating flow of a gas near a stagnation point on a hot wall, *J. appl. Mech.* **38**, 820–828 (1971).
9. L. H. Back, Flow and heat transfer in laminar boundary layers with swirl, *AIAA Jl* **7**, 1781–1789 (1969).

Int. J. Heat Mass Transfer. Vol. 25, No. 2, pp. 293–297, 1982
Printed in Great Britain

0017-9310/82/020293-05 $03.00/0

NATURAL CONVECTION HEAT TRANSFER COEFFICIENTS MEASURED IN EXPERIMENTS ON FREEZING

E. M. SPARROW and P. SOUZA MENDES
Department of Mechanical Engineering, University of Minnesota, Minneapolis, Minnesota 55455, U.S.A.

(*Received* 1 *April* 1981 *and in revised form* 9 *June* 1981)

NOMENCLATURE

g, gravitational acceleration;
h, local heat transfer coefficient at solid–liquid interface;
k, thermal conductivity of liquid phase;
k_s, thermal conductivity of solid phase;
Nu_x, local Nusselt number, hx/k;
n, normal to interface;
Pr, Prandtl number;
Ra_x, local Rayleigh number, $[g\beta(T_0 - T^*)x^3/\nu^2]Pr$;
r, radial coordinate;
r_w, radius of cooled tube;
T, temperature;
T_0, wall temperature of containment vessel;
T_w, wall temperature of cooled tube;
T^*, fusion temperature;
T_∞, temperature outside of boundary layer;
x, axial coordinate measured downward along cooled tube.

Greek symbols

β, coefficient of thermal expansion;
δ, local thickness of frozen layer;
ν, kinematic viscosity.

INTRODUCTION

IT IS NOW well established that natural convection plays a key role in both freezing and melting processes [1]. In the case of freezing, natural convection occurs in the unfrozen liquid into which the solidification front advances, provided that the temperature of the liquid exceeds the phase-change temperature. For melting, natural convection will occur in the liquid melt, except, perhaps, for very thin melt layers where heat is transferred by conduction alone.

For either freezing or melting, the liquid-filled volume in which the natural convection takes place is not of elementary shape (such as, for example, rectangular or annular enclosures). The non-elementary nature of these liquid volumes is related to the fact that at least one of the boundaries of the volume is the phase-change interface. In the presence of natural convection, the interface is, generally, a curved surface which does not coincide with a coordinate surface (e.g., a surface where one of the coordinates is constant). Another feature of the phase-change interface is that its shape may change with time as freezing or melting progresses. As a consequence of the shape of the liquid volume, it appears that the heat transfer coefficients needed for the analysis of natural convection-affected phase change cannot be taken directly from the literature on natural convection in single-phase systems where relatively regularly shaped domains have been considered.

Natural convection heat transfer coefficients specific to melting have been investigated experimentally to a moderate extent and, aside from the recent experiments of [2], this work has been brought together in [1]. In addition, numerical solutions for the conjugate conduction–natural convection problem associated with melting about a vertical cylinder have been carried out [3, 4]. On the other hand, as is apparent from [1], there is a paucity of work on natural convection heat transfer coefficients related to freezing.

The present paper reports on natural convection heat transfer coefficients measured in experiments on freezing about a cooled vertical tube which is situated in a liquid phase-change medium that is maintained at a temperature above the fusion value.

THE EXPERIMENTS

The apparatus used for the experiments is an adaptation of that employed in an earlier study with different objectives [5]. In order to facilitate the subsequent presentation and discussion of the results, it is useful to give a brief description of the apparatus here.

Figure 1 is a schematic drawing of the apparatus with a data run in progress. The main components of the apparatus are: (1) a cylindrical containment vessel for the phase-change medium, (2) a constant temperature water bath which serves as an isothermal environment for the containment vessel and which maintains the surface temperature of the vessel at a constant value T_0 that is higher than the fusion temperature T^*, and (3) a circular tube which is positioned along the axis of the containment vessel during a data run and which is water-cooled so that its surface temperature T_w is lower than

the fusion temperature T^*, thereby causing freezing to occur.

As seen in the figure, the lower part of the containment vessel is fitted with a disk of styrofoam insulation whose purpose is to avoid thermal interactions between the lower portions of the freezing specimen and the bottom wall of the containment vessel. Thermal isolation at the otherwise open top of the vessel is achieved by the use of a styrofoam cap. The containment vessel is supported and positioned in the water bath by a lip which extends radially outward at its upper end; the lip rests on the plexiglass plate which covers the top of the constant temperature bath.

The key dimensions of the apparatus are as follows: (1) inner diameter of the containment vessel, 15.2 cm (6 in.); (2) depth of the liquid phase-change medium in the containment vessel with the water-cooled tube in place, 11.56 cm (4.55 in.); and (3) outer diameter of the cooled tube, 2.49 cm (0.982 in.). The phase-change medium is 99% pure *n*-eicosane paraffin with a fusion temperature of 36.4°C (97.5°F).

In preparation for a data run, the containment vessel and its charge of liquid paraffin were placed in the constant-temperature bath to attain thermal equilibrium at the pre-set temperature T_0. During this period, the water-cooled tube was absent from the containment vessel, and chilled water at temperature T_w was circulated through the tube. Once the liquid phase-change medium had attained a uniform temperature T_0, and the cooled-tube temperature was equal to T_w, the tube was inserted into the containment vessel and the data run initiated.

During any data run, the wall of the containment vessel was maintained at a uniform temperature $T_0 > T^*$. As a consequence, a natural convection flow was set up in the liquid paraffin, the circulation pattern of which is shown schematically in Fig. 1. Owing to the fact that both T_0 and T^* are maintained at fixed values throughout the run, the natural convection flow, once initiated, is sustained (i.e. it does not die away as would occur if the wall of the containment vessel were insulated).

It was demonstrated in [5] that the presence of sustained natural convection in the liquid region retards the freezing process and ultimately causes it to terminate. Thus, after a certain time, which depends on the magnitudes of $(T_0 - T^*)$ and $(T^* - T_w)$, there is no further freezing, even though the tube wall temperature is lower than the fusion temperature. Larger values of $(T_0 - T^*)$ create stronger natural convection circulations and, therefore, give rise to thinner frozen specimens. On the other hand, larger values of $(T^* - T_w)$ increase the radial heat conduction in the solidified material, which leads to thicker specimens.

OBJECTIVES AND OPERATING CONDITIONS

The experiments were aimed at exploring certain features of the natural convection heat transfer coefficient at the solid–liquid interface. The first objective was to determine how the heat transfer coefficient at a given axial station responds to changes of the frozen layer thickness when the thermal driving force for natural convection, $(T_0 - T^*)$, is held fixed. A highly desirable outcome of such a determination would be to find that the coefficient is insensitive to the local layer thickness. This would legitimize the use of a time-independent local heat transfer coefficient in the analysis of the timewise growth of the frozen layer in the presence of sustained natural convection in the liquid.

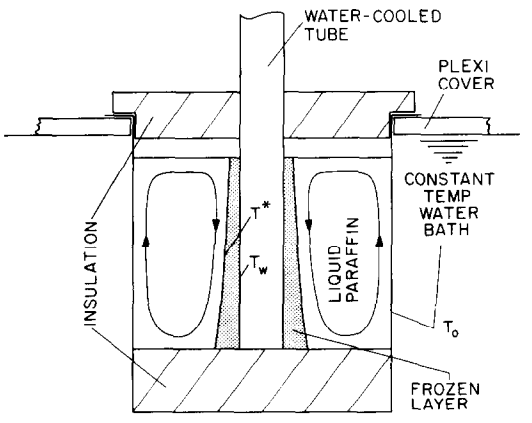

FIG. 1. Schematic of the apparatus with a data run in progress.

To fulfil the aforementioned objective, three series of data runs were made, all with an identical value of the natural convection driving force $(T_0 - T^*)$ equal to 5.56°C (10°F). The three series were respectively characterized by frozen layer temperature differences $(T^* - T_w)$ equal to 8.33, 11.11 and 16.67°C (15, 20 and 30°F). In each series, data runs were made for a succession of increasing run times, and this was continued until no further growth of the frozen layer was detected.

A second objective of the study was to attempt to relate the experimentally determined heat transfer coefficients to literature values for single-phase natural convection.

RESULTS AND DISCUSSION

To illustrate the manner in which the thickness of the frozen layer varies with time at various axial stations, Fig. 2 has been prepared. This figure corresponds specifically to the series of data runs characterized by $(T^* - T_w) = 11.11$°C and $(T_0 - T^*) = 5.56$°C, but it is also typical of the other series. The x coordinate measures axial distances downward from the top of the frozen specimen, while δ is the local thickness of the layer (the thickness measurements were made with a sensitive dial gage). As expected, the thickness of the frozen layer increases rather rapidly with time at first, but the rate of increase slows as time passes and, finally, a terminal thickness is attained.

The terminal thicknesses for all three series of data runs have been plotted in Fig. 3 as a function of the axial coordinate. This figure affirms the statement made earlier in the paper that the presence of natural convection in the liquid gives rise to curved interfaces which do not coincide with coordinate surfaces. It may be seen that the thickness of the frozen layer increases in the direction from the top to the bottom of the specimen. Since thinner frozen layers correspond to higher natural convection heat transfer coefficients [5], Fig. 3 indicates that the coefficient decreases from the top to the bottom of the specimen, which corresponds to the direction of fluid flow along the interface (Fig. 1). Since the natural convection boundary layer grows thicker in the direction of fluid motion, the decrease of the heat transfer coefficient is reasonable. It may also be noted in Fig. 3 that the frozen layer thickness corresponding to the largest value of $(T^* - T_w)$ is almost twice that for the smallest value of $(T^* - T_w)$.

When freezing ceases, the local convective heat transfer from the liquid to the interface is equal to the heat transfer conducted radially † across the frozen layer, provided that axial conduction in the layer can be neglected. The local convective flux can be expressed as $h(T_0 - T^*)$, where h denotes the local heat transfer coefficient. In considering the radial conduction, cognizance must be taken of the temperature dependence of the thermal conductivity k_s of the solid [6]. If it is assumed that k_s can be represented as a linear form (i.e. $k_s = a + bT$) over a small range of temperature, then the radial heat flux at the interface can be written as

$$\bar{k}_s(T^* - T_w)/(r_w + \delta)\ln(1 + \delta/r_w). \quad (1)$$

where $\bar{k}_s$ is the thermal conductivity evaluated at $\bar{T} = \frac{1}{2}(T^* + T_w)$, r_w is the radius of the cooled tube, and δ is the local

† This assumes that $\partial T/\partial n$ at the interface (n = normal) is essentially equal to $\partial T/\partial r$, as will be verified shortly.

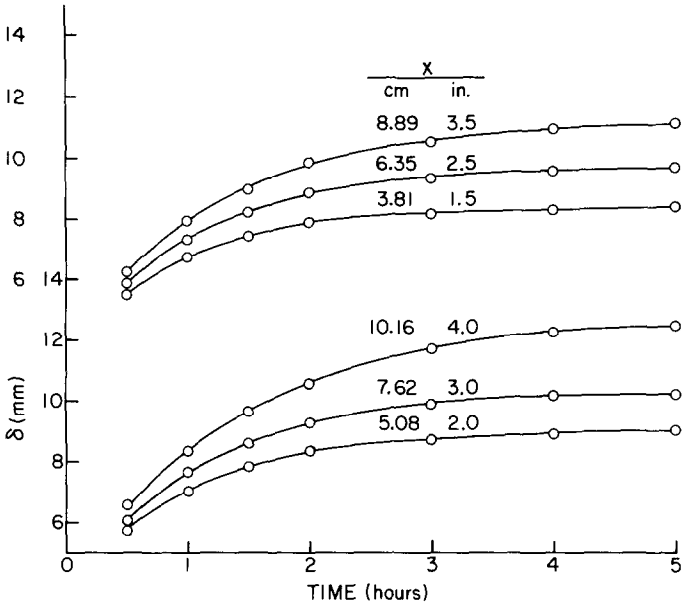

FIG. 2. Variation of the thickness of the frozen layer with time at various axial stations; $(T^* - T_w) = 11.11°C$, $(T_0 - T^*) = 5.56°C$.

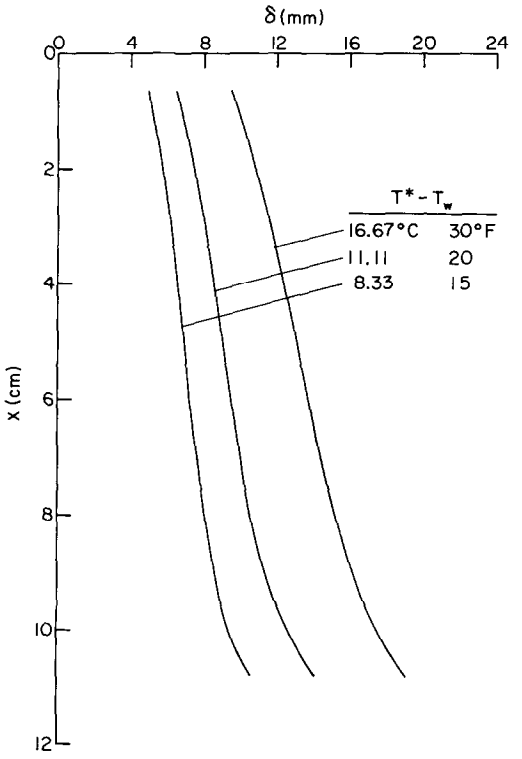

FIG. 3. Terminal thickness distributions.

thickness of the frozen layer. If the heat flux expressed by equation (1) is equated to the local convective heat flux, there follows

$$h = \bar{k}_s[(T^* - T_w)/(T_0 - T^*)]/(r_w + \delta)\ln(1 + \delta/r_w). \quad (2)$$

Numerical results for the local heat transfer coefficient h have been evaluated from equation (2) by introducing the measured terminal thicknesses δ along with the appropriate values of $(T^* - T_w)$ and $(T_0 - T^*)$ and with $\bar{k}_s$ values from [6]. These results are listed in Table 1 as a function of the axial coordinate x for each of the three series of data runs. For compactness, the series are identified as I, II, and III where these symbols are defined at the bottom of the table. Also listed in the table are values of the local Nusselt number defined as $Nu_x = hx/k$, in which the thermal conductivity k of the liquid is from [7]. For reference purposes, it may be noted that the results of Table 1 correspond to a Prandtl number $Pr = 60.5$ and to a Rayleigh number Ra_x at, say, $x = 10.16$ cm (4 in), equal to about 10^8.

Examination of the table shows that at any axial station x, the heat transfer coefficients are virtually the same for the three cases, with the maximum deviations of $1\frac{1}{2}\%$ being well within the accuracy of the experiments. Thus, Table 1 demonstrates that the terminal heat transfer coefficients are independent of the layer thickness at any given axial station and at a fixed thermal driving force $(T_0 - T^*)$.

When the rate of growth of the frozen layer (i.e. $\partial\delta/\partial t$) is very slow, as is true over almost all of the freezing period, then it is reasonable to expect that the natural convection in the liquid region will be quasi-steady, that is, at each moment, an instantaneous steady state exists. Thus, as far as the liquid is concerned, it does not sense any difference between the case of a moving interface and the case of a stationary interface. As a consequence, the conclusions about the influence of δ on the heat transfer coefficient, which have been drawn from terminal state (i.e. steady state) results, also apply to the quasi-steady situation.

From the foregoing, it follows that for the case of sustained natural convection in the liquid, it is permissible to use steady state heat transfer coefficients for the analysis of the major portion of the freezing period. This outcome may be regarded as the most interesting finding of this study.

It is appropriate to explore briefly the reasons for the insensitivity of the heat transfer coefficient h to the layer thickness δ. If h were to be sensitive to δ, the sensitivity would be caused by the following factors: (1) changes in transverse curvature, (2) changes in longitudinal curvature, and (3) changes in the size of the annular gap between the solid–liquid interface and the wall of the containment vessel. The transverse curvature effect for natural convection boundary layer flow along a vertical cylinder was evaluated in [8] for a wide range of Prandtl numbers and Grashof numbers. By interpolating in Table 1 of [8] and using the operating conditions of the present experiments, it was estimated that the transverse curvature effects were, at most, in the 1–2% range.

To assess possible effects due to longitudinal curvature, the derivative $\partial\delta/\partial x$ was locally evaluated from the measured data for δ vs x. From these, it was found that the maximum inclination of the interface relative to the vertical was about 10°. An estimate of the main effect of longitudinal curvature can be obtained by replacing the gravitational acceleration g with $g(\cos\theta)$, where θ is the inclination angle. Furthermore, the heat transfer coefficient responds to the gravitational acceleration approximately as $g^{1/4}$. Then, since $(\cos 10°)^{1/4} = 0.996$, it appears that longitudinal curvature effects are fully negligible.

The next issue relates to the possible effects of changes in the size of the annular gap between the solid–liquid interface and the wall of the containment vessel. In the absence of the frozen layer, the radial gap between the cooled tube and the wall of the vessel is 63.5 mm. Thus, the gap which remains at the termination of freezing is determined by subtracting the δ values of Fig. 3 from 63.5. From this, it is seen that for the three cases considered, there are moderate differences in the various gap sizes at any given axial station.

In exploring the importance of these differences, the literature was examined with a view to finding natural convection heat transfer results for vertical annular enclosures with given temperatures on the inner and outer cylindrical surfaces. Some results are available in [9, 10], but the maximum Rayleigh number considered there is about two orders of magnitude smaller than that of the present experiments. More recent references, e.g. [11], deal with vertical annular gaps where the end faces are thermally active rather than the cylindrical surfaces and, therefore, are not applicable to the present situation. In lieu of other information, some guidance may be taken from the authors' own work on natural convection in melt cavities [2, 12]. There, it was found that the natural convection heat transfer coefficient was essentially independent of the cavity size for inter-wall dimensions on the order of those of the present experiments.

The foregoing discussion serves to buttress the experimentally encountered insensitivity of the heat transfer coefficient to the thickness of the frozen layer. It still remains, however, to justify the neglect of the difference between the normal and radial temperature derivatives at the interface, as employed in the derivation of equation (2). In this connection, it is readily shown that

$$\partial T/\partial n = [1 + (\partial\delta/\partial x)^2]^{1/2}(\partial T/\partial r). \quad (3)$$

From the measured values of δ vs x, the factor multiplying $\partial T/\partial r$ was evaluated. At almost all axial stations, the deviation of this factor from one was under 1%; at $x = 10.16$ cm (4 in.), values as large as $1\frac{1}{2}\%$ were encountered, but the differences between the three cases (I, II, and III of Table 1) were less than $\frac{1}{2}\%$. In the light of this, it is justifiable to neglect the differences between the radial and normal derivatives.

It is appropriate to attempt to relate the heat transfer coefficients and Nusselt numbers of Table 1 with literature information. The geometrical configuration which, in the available literature, most closely approximates the shape of the liquid region of the present experiments is the vertical

Table 1. Measured values of h and Nu_x

x (c)	h (W/m² – °C) I	II	III	Nu_x I	II	III
3.81	60.7	61.3	61.6	15.2	15.3	15.4
5.08	56.3	56.4	56.7	18.8	18.8	18.9
6.35	52.8	52.4	52.5	22.0	21.8	21.9
7.62	48.7	49.1	48.3	24.4	24.6	24.2
8.89	44.2	44.1	44.1	25.8	25.8	25.7
10.16	38.5	38.4	38.8	25.7	25.6	25.9

I, II, III → $(T^* - T_w) = 8.33, 11.11, 16.67$°C.

concentric annulus. However, as already noted, the published heat transfer results for the annulus are confined to Rayleigh numbers that are smaller than those encountered here.

Although they may not be strictly applicable, it was thought that the heat transfer coefficients for an isothermal vertical plate might form an interesting basis of comparison with the present data. In this connection, it is necessary to take cognizance of the fact that the vertical-plate results are based on the temperature difference $(T_\infty - T^*)$, where T_∞ is the temperature of the fluid outside the boundary layer. In contrast, the present h values are based on $(T_0 - T^*)$. With this in mind, the classical vertical-plate Nusselt number prediction, specialized to $Pr = 60.5$ by interpolation in Table 1 of [13], can be written as

$$Nu_x = 0.486 Ra_x^{1/4}[(T_\infty - T^*)/(T_0 - T^*)]^{5/4} \quad (4)$$

where both Nu_x and Ra_x correspond to $(T_0 - T^*)$.

In applying equation (4) to the present situation, T_∞ will be interpreted as the temperature of the liquid which lies between the boundary layers which respectively flow upward along the wall of the containment vessel and downward along the solid–liquid interface. Measurements of T_∞ at mid-height yielded a value $(T_\infty - T^*)/(T_0 - T^*) \sim 0.85$, so that the numerical constant multiplying $Ra_x^{1/4}$ in equation (4) becomes equal to 0.397.

When equation (4) is evaluated at the successive x values listed in Table 1, the corresponding Nu_x values are 19.2, 23.9, 28.3, 32.5, 36.4 and 40.3. While these results are generally high compared with those of Table 1, the level of agreement is quite satisfactory when account is taken of the significant geometrical differences between the systems being compared.

Acknowledgement—This research was performed under the auspices of the Office of Basic Energy Sciences of the U.S. Department of Energy (DOE/DE-AC02-79ER10343).

REFERENCES

1. R. Viskanta, A. G. Bathelt and N. W. Hale, Jr., Latent heat-of-fusion energy storage: experiments on heat transfer during solid–liquid phase change, *Proceedings, Third Miami International Conference on Alternative Energy Sources*, December 1980.
2. R. G. Kemink and E. M. Sparrow, Heat transfer coefficients for melting about a vertical cylinder with or without subcooling and for open or closed containment, *Int. J. Heat Mass Transfer* **24**, 1699–1710 (1981).
3. E. M. Sparrow, S. V. Patankar and S. Ramadhyani, Analysis of melting in the presence of natural convection in the melt region, *J. Heat Transfer* **99**, 521–526 (1977).
4. L. M. Hossfeld, A coordinate transformation method for solving a convection phase change problem. Ph.D. thesis, Department of Mechanical Engineering, University of Minnesota, Minneapolis, Minnesota (1979).
5. E. M. Sparrow, J. W. Ramsey and R. G. Kemink, Freezing controlled by natural convection, *J. Heat Transfer* **101**, 578–584 (1979).
6. E. I. Griggs and D. W. Yarbrough, Thermal conductivity of solid unbranched alkanes from *n*-hexadecane to *n*-eicosane, *Proc. 14th Southeastern Seminar on Thermal Sciences*, 256–267 (1978).
7. E. I. Griggs and W. R. Humphries, A design handbook for phase change thermal control and energy storage devices, NASA Technical Paper 1074 (1977).
8. T. Cebeci, Laminar free convection heat transfer from the outer surface of a slender vertical circular cylinder, *Proc. 5th International Heat Transfer Conference*, paper NC14, Vol. III, pp. 15–19 (1974).
9. G. de Vahl Davis and R. W. Thomas, Natural convection between concentric vertical cylinders, *Phys. Fluids* **12**, Suppl. II, 198–207 (1969).
10. R. W. Thomas and G. de Vahl Davis, Natural convection in annular and rectangular cavities—a numerical study, *Proc. 4th International Heat Transfer Conference*, paper NC2.4, Vol. IV (1970).
11. H. Ozoe, T. Shibata and S. W. Churchill, Natural convection in an inclined circular cylindrical annulus heated and cooled on its end plates, *Int. J. Heat Mass Transfer* **24**, 727–737 (1981).
12. E. M. Sparrow, R. R. Schmidt and J. W. Ramsey, Experiments on the role of natural convection in the melting of solids, *J. Heat Transfer* **100**, 11–16 (1978).
13. A. J. Ede, Advances in free convection, *Adv. Heat Transfer* **4**, 1–64 (1967).